Cell. Mol. Life Sci. 63 (2006) 0100–0111
1420-682X/06/010100-12
DOI 10.1007/s00018-005-5512-6


Cellular and Molecular Life Sciences

# Research Article

# Role of the conserved glutamine 291 in the rat γ-aminobutyric acid transporter rGAT-1

**S. A. Mari[a], A. Soragna[b], M. Castagna[a], M. Santacroce[a], C. Perego[a], E. Bossi[b], A. Peres[b] and V. F. Sacchi[a, *]**

[a] Institute of General Physiology and Biological Chemistry 'G. Esposito', University of Milan, Via Trentacoste 2, 20134 Milano (Italy), Fax: +390250315775, e-mail: franca.sacchi@unimi.it
[b] Laboratory of Cellular and Molecular Physiology, Department of Structural and Functional Biology and Center for Neuroscience, University of Insubria, 21100 Varese (Italy)

Received 24 October 2005; accepted 11 November 2005
Online First 27 December 2005

**Abstract.** We investigated the role of the Q291 glutamine residue in the functioning of the rat γ-aminobutyric acid (GABA) transporter GAT-1. Q291 mutants cannot transport GABA or give rise to transient, leak and transport-coupled currents even though they are targeted to the plasma membrane. Coexpression experiments of wild-type and Q291 mutants suggest that GAT-1 is a functional monomer though it requires oligomeric assembly for membrane insertion. We determined the accessibility of Q291 by investigating the impact of impermeant sulfhydryl reagents on cysteine residues engineered in close proximity to Q291. The effect of these reagents indicates that Q291 faces the external aqueous milieu. The introduction of a steric hindrance close to Q291 by means of [2-(trimethylammonium)ethyl] methanethiosulfonate bromide modification of C74A/T290C altered the affinity of the mutant for cations. Taken together, these results suggest that this irreplaceable residue is involved in the interaction with sodium or in maintaining the cation accessibility to the transporter.

**Key words.** Neurotransmitter transporter; GAT-1; electrophysiology; site-directed mutagenesis; *Xenopus laevis* oocyte; structure-function relationship.

γ-Aminobutyric acid (GABA) is the major inhibitory neurotransmitter in mammalian brain, and the GABA transporter GAT-1 is an integral membrane protein responsible for the reuptake of GABA from the synaptic cleft during neurotransmission. GAT-1 was the first cloned member of a large family of homologous proteins, the $Na^+/Cl^-$-dependent neurotransmitter transporters [1], which includes transporters for other neurotransmitters such as norepinephrine, dopamine, serotonin and glycine, as well as for a number of other substrates that share the common property of being amino acids or amino acid derivatives [2]. These membrane proteins are predicted to have 12 transmembrane-spanning domains (TMDs) linked by hydrophilic loops with the $NH_2$ and COOH terminals inside the cell, a topological model that has been confirmed for the serotonin transporter by means of site-directed chemical labeling [3]. GAT-1 mediates the electrogenic reuptake of GABA in the presence of sodium and chloride ions by means of a mechanism that has been extensively studied [4–12].

Many attempts have been made to determine which of the transporter amino acid residues are involved in the interaction with GABA and with $Na^+$ and $Cl^-$ ions, and which participate in the conformational changes associated with translocation [13–15]. As GABA is a zwitterionic molecule and its cosubstrates are charged species, the first studies focused on the charged and conserved residues predicted to be located in (or adjacent to) the transmembrane (TM) domains. This allowed the identification of

* Corresponding author.

two charged residues that are critical for GAT-1: arginine 69 [16] and glutamate 101 [17]. A different approach investigated the possible role of aromatic residues through the interaction of their $\pi$ electrons with positively charged substrates such as $Na^+$ or the amino group of the neurotransmitter [18–20]. A number of tryptophan residues residing within the membrane domain of the GABA transporter have been investigated [21]. Tryptophan 68 was initially believed to interact with the amino group of the neurotransmitter, but a subsequent and more detailed analysis revealed its involvement in cation binding [22]. Cysteines introduced at positions 68 (TMD 1) and 143 (TMD 3) have recently been shown to be in close proximity within the transporter monomer, thus supporting the idea that the binding determinants for the substrate in GAT-1 are located in TMD 1 and 3 [23]. Analysis of the tyrosine residues of GAT-1, predicted to be located in the membrane, and conserved throughout the family, has shown that tyrosine 140 is critical for neurotransmitter recognition [24].

We investigated the role in GAT-1 function of glutamine 291 which, according to secondary-structure prediction algorithms, is located at the extracellular membrane surface. Despite their rare presence in TM helices, polar residues are often highly conserved in multispanning TM proteins [25], which suggests that they provide functionally and/or structurally required molecular interactions, and that evolutionary pressure prevents their substitution in related proteins in different organisms. Q291 is strictly conserved in all members of the family including bacterial and archaeal proteins, indicating that it may play a fundamental role in the function of these transporters.

Our experiments confirmed the topological prediction of Q291 on the extracellular membrane surface and its crucial role in GAT-1 function. Q291 mutants, although inserted into the plasma membrane, are unable to transport measurable amounts of GABA or to elicit any of the currents shown by the wild-type (WT) transporter. A defect in the recognition of the organic substrate cannot explain all the experimental data and a defect in quaternary protein folding cannot be envisaged. Our hypothesis is that Q291 may play a fundamental role in the initial interaction of the transporter with sodium, which would obviously involve other critical residues at the protein membrane surface. Our data do not necessarily indicate a direct role for Q291 in cation binding, but Q291 may be fundamental to maintain the conformational integrity of an external region of the transporter that makes it accessible to the cation. Very recently, the first structure of a member of the $Na^+/Cl^-$-dependent neurotransmitter transporter family was solved. Yamashita et al. [26] reported the crystal structure of the leucine transporter $LeuT_{Aa}$ from the bacterium *Aquifex aeolicus*. This structure represents a conformation of the transporter in which the binding pocket is occluded and the external and internal gates are closed. The molecular interactions of $LeuT_{Aa}$ Q250, which corresponds to GAT Q291 (fig. 1A), are clearly shown and compatible with our data concerning the role of Q291 in GAT function.

## Materials and methods

**Site-directed mutagenesis.** The oocyte expression vector pAMV-PA containing rGAT-1 cDNA was a generous gift from H. A. Lester and C. Labarca (Division of Biology, California Institute of Technology, Pasadena, Calif.). The mutants were synthesized by PCR using the Quick Change Site-Directed Mutagenesis Kit (Stratagene), and the mutations were confirmed by DNA sequencing.

**Oocyte expression of WT and mutated transporters.** The oocyte expression vector pAMV-PA containing WT or mutant GAT-1 cDNA was *Not*I digested, *in vitro* capped, and transcribed using T7 RNA polymerase (Stratagene). The oocytes were collected as previously described [27], and injected with 12.5 ng cRNA in 50 nl of water using a manual microinjection system (Drummond). The oocytes were incubated at 18 °C for 3–4 days in Barth's solution supplemented with 50 µg/ml gentamicin and 2.5 mM sodium pyruvate before the experiments.

**Transport experiments.** GABA uptake was measured 3 days after injection. Groups of 10–12 oocytes were incubated in 100 µl uptake solution (100 mM NaCl, 2 mM KCl, 1 mM $CaCl_2$, 1 mM $MgCl_2$, 10 mM HEPES/Tris, pH 7.5) with 100 µM [$^3$H]GABA (1000 KBq/ml) for 60 min. The oocytes were then rinsed with ice-cold wash solution (100 mM choline chloride, 2 mM KCl, 1 mM $CaCl_2$, 1 mM $MgCl_2$, 10 mM HEPES/Tris, pH 7.5) and dissolved in 250 µl of 10% SDS for liquid scintillation counting. GAT-1-mediated transport was plotted as the difference between the mean uptake measured in cRNA-injected oocytes and that observed in non-injected oocytes.

**Inhibition studies with sulfhydryl reagents.** Before the uptake experiments and unless otherwise indicated, the oocytes were incubated at room temperature with 2 mM of the cysteine-modifying reagents MTSET and sodium (2-sulfonatoethyl) methanethiosulfonate [$\alpha$-(trimethylammonium)ethyl]methanethiosulfonate bromide (MTSES) for 15 min in Barth's solution, subsequently rinsed with the wash solution, and then incubated for uptake measurements. In electrophysiological experiments, the same oocytes were tested before sulfhydryl modification and then again after methanethiosulfonate (MTS) incubation (under the same conditions as used in the uptake studies). In this way, each oocyte was its own control.

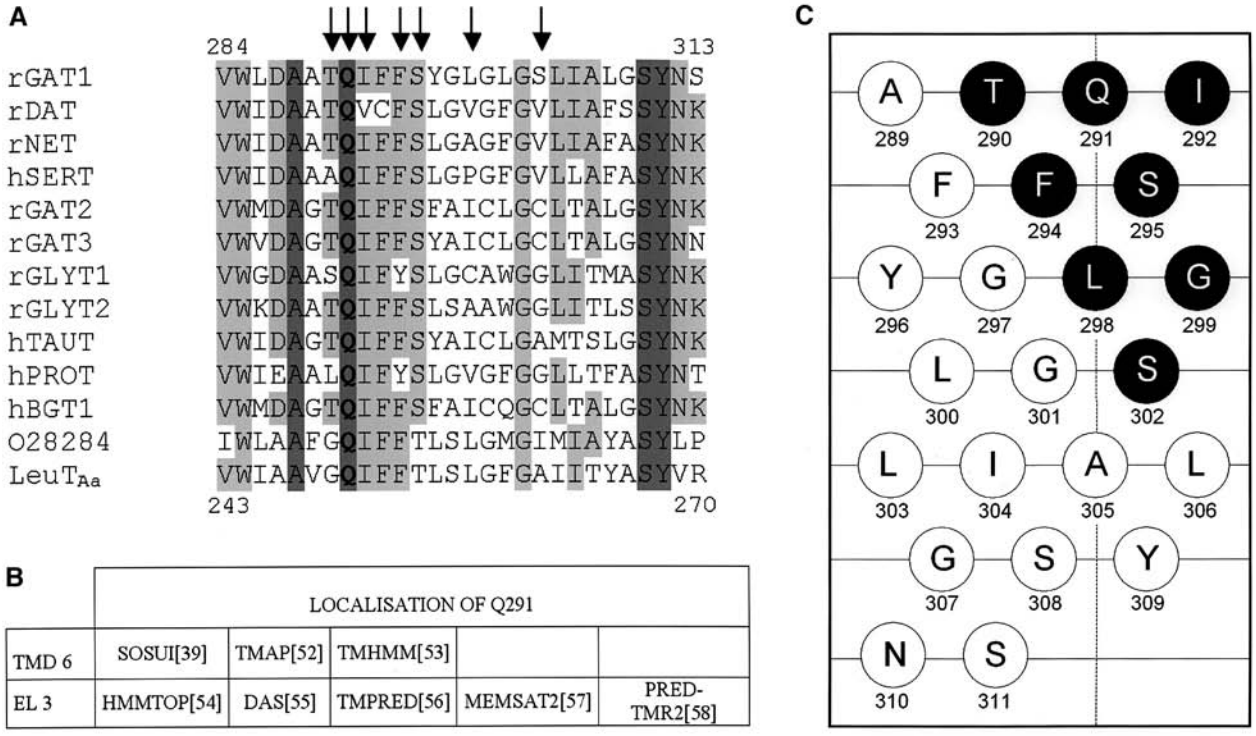


Figure 1. Sequence conservation of the region including TMD 6 within different $Na^+/Cl^-$-dependent neurotransmitter transporters, topological prediction of Q291 and representation of the GAT-1 TM helix 6. (*A*) The first row shows amino acid residues 284–313 according to rGAT-1 numbering, and the last acid residues 243–270 according to *A. aeolicus* $LeuT_{Aa}$ numbering (see Discussion for further details). Sequence similarity with GAT-1 of the homologues from archaeal, bacterial and mammalian sources is shown. The arrows indicate the residues mutated in this study. Q291 is indicated in bold. (*B*) Assignment of Q291 to the C termini of the third extracellular loop or the N termini of TMD 6 according to different secondary-structure prediction algorithms. (*C*) The secondary structure prediction system for membrane proteins SOSUI [39] assigns the sequence of 23 amino acids ATQIFFSYGLGLGSLIALGSYNS from 289 to 311 of GAT-1 to TMD 6. The residues mutated in this study are shown in black circles.

**Electrophysiology.** Classical two-electrode voltage clamp experiments were performed using GeneClamp (Axon Instruments), or Oocyte Clamp OC-725B (Warner Instruments) amplifiers. Reference electrodes were connected to the experimental oocyte chamber via agar bridges (3% agar in 3 M KCl) to minimize the effects of chloride on junction potential. Borosilicate electrodes with a tip resistance of 0.5–2 MΩ were filled with 3 M KCl. The holding potential was kept at –40 mV, and 400-ms voltage pulses were applied in the voltage range –140 mV to 40 mV in 20-mV increments. Four pulses were averaged at each potential; signals were filtered at 1 KHz and sampled at 2 KHz. The experimental protocols, data acquisition and analysis were performed using pClamp software (Axon Instruments), and all of the figures were prepared using Origin 5.0 software (Microcal Software). The external solution consisted of (in mM): NaCl98, LiCl98, TMACl (tetramethylammonium chloride) or NMDG (N-methyl-D-glucamine) 98, $MgCl_2$ 1, $CaCl_2$ 1.8, HEPES 5; pH was adjusted to a final value of 7.6 by adding NaOH, LiOH, TMAOH or HCl. In the experiments using reduced sodium concentrations, the cation was iso-osmotically replaced by $TMA^+$ or NMDG. To induce transport-associated currents, GABA was added at a final concentration of 100 μM, unless otherwise stated. The transport-associated currents were estimated by subtracting the traces in the absence of GABA from those in its presence under each experimental condition. The experiments investigating the sodium-induced inhibition of lithium currents were performed using 96 mM lithium in the presence of 2 mM sodium. To maintain osmolarity in the control solution, 2 mM NMDG were added to 96 mM lithium. To isolate the pre-steady-state currents, the specific rGAT-1 blocker, 1-(4,4-diphenyl-3-butenyl)-3-piperidine carboxylic acid hydrochloride (SKF89976A) (Tocris), was used at a final concentration of 30 μM. All of the experiments were performed at room temperature.

**Cell surface biotinylation.** The cell surface expression of GAT-1 and the mutants was tested using a membrane-impermeant reagent, EZ-Link Sulfo-NHS-SS-Biotin (Pierce). Groups of five to ten oocytes were rinsed three times with ice-cold PBS, pH 8, and then incubated twice on ice in 750 μl PBS containing EZ-Link Sulfo-NHS-SS-

Biotin (1.3 mg/ml) for 15 min. After labeling, the oocytes were rinsed with ice-cold PBS, incubated in 50 mM glycine in PBS for 15 min on ice in order to quench the unreacted biotinylation reagent, and then dissolved in lysis buffer (in mM: NaCl 150, Tris/HCl 20, pH 7.6, 1% Triton X-100, EDTA 5) supplemented with 10 µl/ml of the protease inhibitors leupeptin and aprotinin by means of gentle shaking on ice for 40 min. The solubilized oocytes were centrifuged for 15 min at 13,000 g, and the biotinylated proteins were recovered from the supernatant solution by adding 50 µl ImmunoPure Immobilised Streptavidin beads (Pierce), and incubating for 1.5 h with gentle agitation on ice. The beads were then washed twice with lysis buffer and once with 50 mM TrisHCl, pH 7.5. The final pellets were resuspended in the appropriate SDS sample buffer and incubated for 2 min at 100 °C before being loaded onto an 8–10% polyacrylamide gel for SDS/PAGE. Total samples were obtained by heating 1/10 of the lysates in SDS sample buffer at 100 °C for 2 min, followed by SDS-PAGE. After SDS-PAGE, the proteins were transferred to nitrocellulose and GAT-1 was detected by means of ECL (Amersham) using an affinity-purified antibody to the COOH-terminal tail of GAT-1 at a 1:1500 dilution and horseradish peroxidase-conjugated secondary antibody at a 1:10,000 dilution. All of the antibody, blocking and washing solutions contained 5% milk to minimize the appearance of non-specific bands. The cell surface expression of GAT Q291 mutants was quantified by means of densitometric analysis using Scion Image software.

## Results

**Analysis of Q291 mutants.** A sequence-alignment analysis of about 250 proteins belonging to the family of $Na^+$/$Cl^-$-dependent neurotransmitter transporters (ranging from prokaryotes to human proteins) identified the most conserved residues of the family (see fig. 1 for an extract of this analysis). One of the three most conserved residues was Q291 (GAT-1 numbering), as 97.5% of the sequences have a glutamine residue in the corresponding position. According to secondary-structure prediction algorithms, GAT-1 Q291 is located on the $NH_2$-terminal side of the sixth TM domain or on the COOH-terminal portion of the third extracellular loop (fig. 1B).

To investigate the role of glutamine 291 in GAT-1 function, we used site-directed mutagenesis to delete the residue or replace it with different amino acids. The mutant proteins were expressed in *Xenopus laevis* oocytes and compared with the WT transporter. The deletion of Q291 or its substitution by the amino acids leucine, asparagine or glutamate caused a complete loss of function. None of the mutants was capable of transporting GABA (fig. 2A), and electrophysiological measurements showed

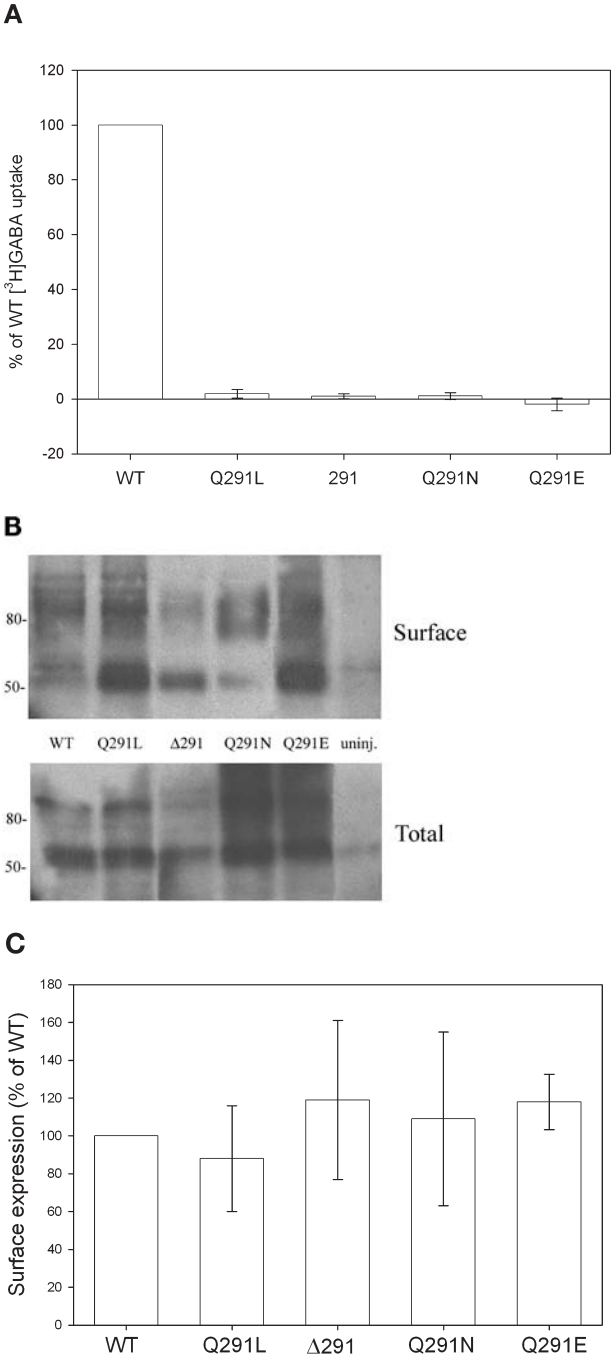


Figure 2. Transport activity and cell surface expression of WT GAT-1 and Q291 mutants. (*A*) Sodium-dependent 100 µM [$^3$H]GABA uptake in *Xenopus* oocytes expressing WT GAT-1 and the mutants Q291L, *Δ*291, Q291N and Q291E. The uptake value is expressed as the percentage of transport activity of WT GAT-1. Mean values ± SE of 10–12 oocytes in at least three independent experiments. (*B*) Surface biotinylation of *Xenopus* oocytes expressing WT and mutated proteins. The GAT-1- and mutant-expressing oocytes were treated as described in Materials and methods. The image shows the biotinylated and total samples of WT, Q291L, *Δ*291, Q291N, Q291E and uninjected oocytes. The positions of standard molecular mass are indicated on the left. (*C*) Cell surface expression of GAT-1 Q291 mutants quantified by densitometry. The data are expressed as the % of WT GAT-1 surface expression; mean values + SE of at least three different experiments.

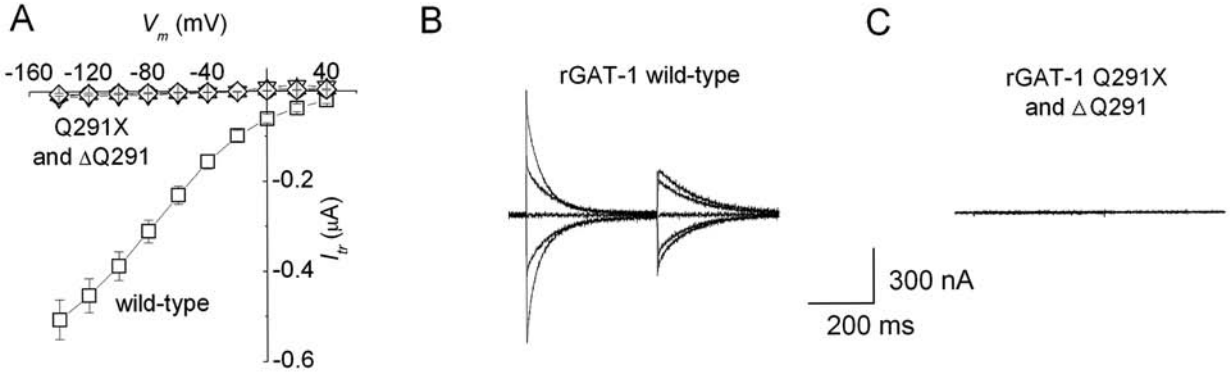


Figure 3. Electrophysiological characterization of WT and mutated GAT-1. (*A*) Current *vs* voltage relationships of the transport-associated current elicited by 100 μM GABA in WT GAT-1 (squares), and the mutants Q291E (downward-pointing triangles), Q291L (upward-pointing triangles), Q291N (circles) and *Δ*291 (diamonds). None of these mutants gave rise to a transport-associated current. Mean values ± SE from eight to ten oocytes from three different batches. (*B*, *C*) Sample traces showing pre-steady-state currents for WT GAT-1 (*B*) and the indicated mutants (X stands for E, L and N in *C*). None of the mutated forms showed pre-steady-state currents. The traces were obtained as explained in Materials and methods. Only the steps from –120 mV to +40 mV are shown (in 40-mV increments).

that they were unable to generate transport-coupled currents (fig. 3A), pre-steady-state currents (fig. 3C) or lithium leak currents (data not shown).

As the complete absence of transport activity and of the currents characterizing the WT transporter may have been due to inefficient targeting to the plasma membrane, the cell surface expression of the mutants was tested using a membrane-impermeant biotinylation reagent, EZ-Link Sulfo-NHS-SS-Biotin. Figure 2B shows the amounts of biotinylated and total WT GAT-1 and mutant proteins (Q291L, *Δ*291, Q291N and Q291E). As previously reported, WT GAT-1 [28] and the mutants were represented by a ≈60-kDa band and an upper band compatible with a dimeric aggregate of the transporter. The specificity of the antibody is shown by the lack of labeling in the control lanes, which represent samples prepared from uninjected oocytes. All of the mutant proteins reached the plasma membrane, which indicates that the deletion or substitution of Q291 did not impair GAT-1 cell surface targeting and thus ruled out the hypothesis of defective targeting as the cause of their lack of activity.

**Coexpression experiments.** Transport proteins are frequently oligomers [29], but the significance of the protein quaternary structure in transport activity has been elucidated in only a few cases. With the exception of glycine transporters [30], most neurotransmitter transporters form constitutive oligomers. GAT-1 oligomers have been visualized in living cells by means of fluorescence resonance energy transfer (FRET) microscopy [31], and some interaction motifs have been shown to support the association of TM domains in GAT-1 and related transporters [32–36]. The characteristics of the Q291 mutants made them good candidates for coexpression experiments designed to investigate the role of GAT-1 oligomerization, because they are non-functional but expressed at the cell surface and also capable of quaternary assembly (fig. 2B). The involvement of Q291 in oligomerization can also be excluded by evidence that the export of GAT-1 and other members of the family to the plasma membrane is dependent on oligomerization (see Discussion).

If the transporter functions only as an oligomer, the coexpression of WT and a correctly inserted non-functional mutant should impair the transport activity of the WT. The coinjection of equal, non-saturating amounts of WT and mutant GAT-1 cRNAs did not have any appreciable effect on WT-mediated GABA transport (fig. 4), even after the coinjection of the WT and mutant in a 1:2 ratio which could possibly favor the effect of the mutant on the WT (data not shown). This was observed after the coexpression of WT GAT-1 with the mutants Q291L, *Δ*291, Q291N and Q291E, as well as with the mutant Y140F which is known to be expressed at the cell surface but is non-functional [24]. As these mutants are not retained intracellularly and are capable of quaternary assembly, their coexpression with the WT should produce a mixture of oligomers consisting of pure WT, pure mutated, and heteromeric oligomers. The absence of any effect of mutant coexpression on WT transport activity indicates that a pure WT oligomer is not required for sodium-coupled GABA transport; in other words, although it requires oligomeric assembly for efficient surface targeting, GAT-1 seems to be a functional monomer.

**Accessibility studies.** In an attempt to elucidate the role of Q291 further, we studied its accessibility by testing the impact of impermeant sulfhydryl-modifying reagents on engineered cysteine residues. This was done using the C74A mutant because this residue is the only external cysteine of GAT-1 affected by impermeant MTS reagents [14, 37, 38]. As the C74A/Q291C mutant is devoid of transport activity (fig. 5), as well as transient, leak and

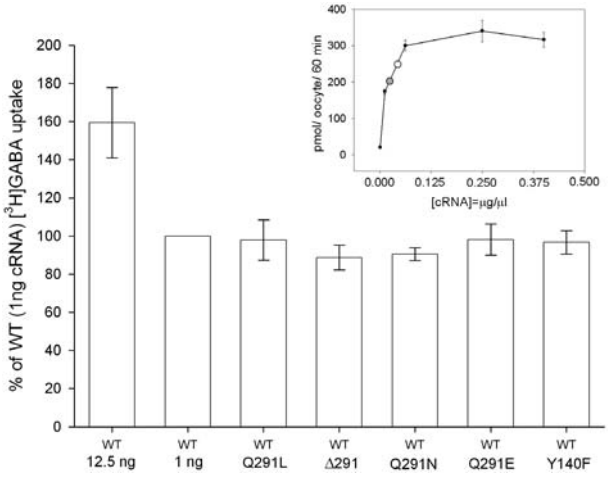


Figure 4. Coexpression of WT GAT-1 and mutants Q291L, Δ291, Q291N, Q291E and Y140F. [3H]GABA uptake at a concentration of 100 µM mediated by WT and the indicated WT/mutant pairs. From left to right, the oocytes were injected with 12.5 ng of WT cRNA (concentration 0.250 µg/µl), 1 ng of WT cRNA (concentration 0.02 µg/µl) and 1 ng WT cRNA mixed with 1 ng of the indicated mutated cRNAs (ratio 1:1). The uptake values are expressed as the percentage of transport activity measured in the oocytes injected with 1 ng WT GAT-1 cRNA (concentration 0.02 µg/µl). Mean values ± SE of groups of 10–12 oocytes in at least three independent experiments. Insert: relationship between 100 µM [3H]GABA uptake and the concentrations of the injected WT GAT-1 cRNA (0.02 µg/µl, grey circle; 0.04 µg/µl, white circle) corresponding to 1 and 2 ng. Mean values ± SE of groups of 10–12 oocytes.

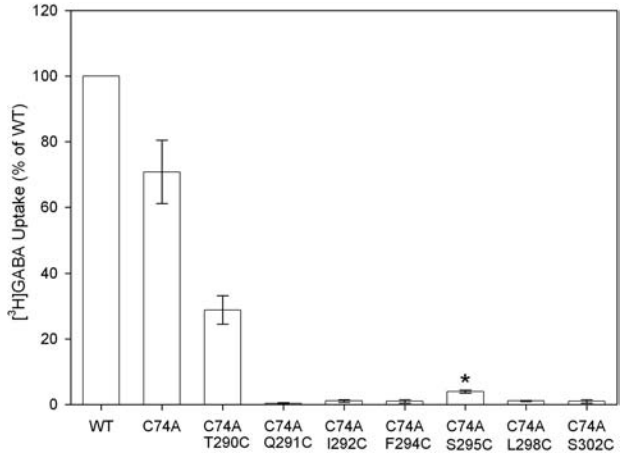


Figure 5. GABA transport mediated by cysteine mutants. [3H]GABA uptake at a concentration of 100 µM as mediated by the C74A, C74A/T290C, C74A/Q291C, C74A/I292C, C74A/F294C C74A/S295C, C74A/L298C and C74A/S302C mutants, expressed as the percentage of transport activity shown by WT GAT-1. Mean values ± SE of 10–12 oocytes in at least three independent experiments. *, significantly different from non-injected oocytes (Student's t test, $p < 0.05$).

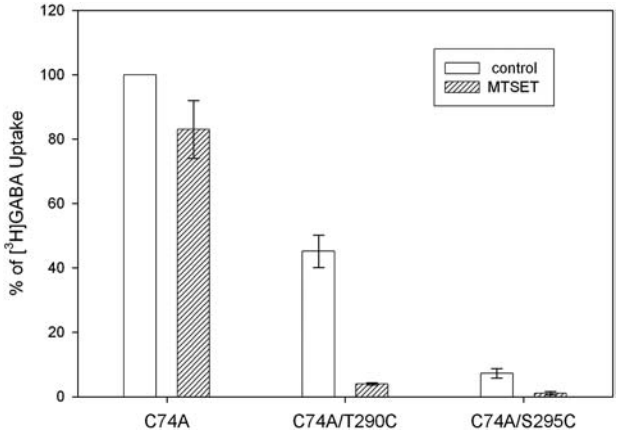


Figure 6. MTSET effect on [3H]GABA uptake induced by GAT-1 C74A, C74A/T290C and C74A/S295C mutants. 100 µM [3H]GABA uptake expressed as the percentage of C74A mediated by the indicated mutants. The white bars represent control conditions (oocytes untreated with the modifying reagent), and the hatched bars, the transport activity after 15 min incubation with MTSET at a concentration of 2 mM. Mean values ± SE of 10–12 oocytes in at least three independent experiments.

transport-associated currents (data not shown), we could not perform any functional test to monitor the effect of impermeant MTS reagents on it. Furthermore, the accessibility of the cysteine introduced into the C74A/Q291C mutant could not be determined using the cysteine-specific biotinylation reagent MTSEA-biotin (N-biotinylaminoethylmethanethiosulfonate) as WT GAT-1 and also the C74A/C399A mutant, lacking the main targets of both permeant and impermeant MTS reagents [13], are labeled by MTSEA-biotin. This result indicates that this reagent can modify other endogenous cysteines [38].

We therefore could not obtain any direct data concerning the external aqueous accessibility of Q291, although the presence of a highly hydrophilic residue such as glutamine in this position suggests that it should have aqueous accessibility. In an attempt to overcome this obstacle, we tested the external aqueous accessibility of the region in which Q291 is located by inserting cysteine residues in proximity to Q291 on the C74A background to produce the double mutants C74A/T290C, C74A/I292C, C74A/F294C, C74A/S295C, C74A/L298C and C74A/S302C (figs. 1A, C). The cysteines F294C, S295C, L298C and S302C were inserted downstream of Q291 and, according to the SOSUI secondary-structure prediction algorithm, are predicted to face the same side of a putative $\alpha$-helix of TMD 6 just below Q291 [39] (fig. 1C). Transport activity could be measured in two of the six double mutants, C74A/T290C and C74A/S295C (fig. 5), which showed reduced uptake and smaller transport-coupled currents (data not shown) in comparison with the WT form. Preincubation with the positively charged MTSET (2 mM for 15 min) caused an 80% inhibition of uptake in C74A/T290C, and 90% in C74A/S295C (fig. 6, hatched bars); similar inhibition was also observed after 10 min pre-incubation with 150 µM MTSET (data not shown). Under

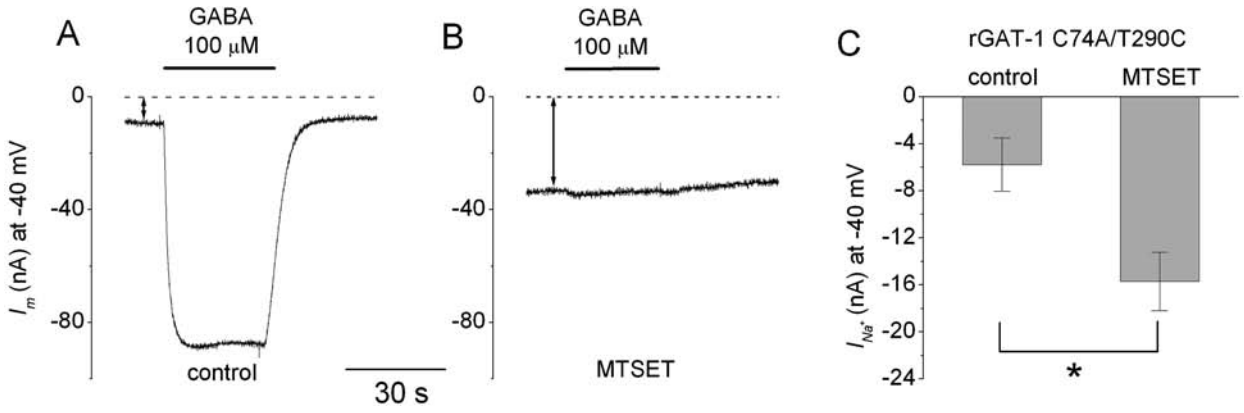


Figure 7. Effect of MTSET on transport-associated and sodium leakage currents of the C74A/T290C double mutant. (*A*, *B*) Sample traces of transport-associated and sodium leakage currents recorded at –40 mV in an oocyte expressing the C74A/T290C mutant before (*A*) and after (*B*) incubation with MTSET. GABA was added at the time indicated by the black bars. The dashed lines represent zero current level, and the arrows indicate the sodium leakage current. (*C*) Evaluation of sodium leakage current under control conditions and after MTSET treatment (n=8) recorded at –40 mV: the values are significantly different (*Student's t test, $p < 0.05$).

both conditions, the $Na^+$ and GABA substrates did not affect MTSET sensitivity (data not shown). The negatively charged MTSES (2 mM pre-incubation for 15 min), whose size is similar to that of MTSET, had the same effect (data not shown).

The inhibition of these mutants (which respectively expose a cysteine residue just before and one helix turn below Q291) by impermeant MTS reagents suggests that the hydrophilic Q291 is accessible from the external aqueous milieu. One possible explanation for this inhibition is that the C74A/T290C and C74A/S295C mutants may expose an endogenous and previously inaccessible cysteine residue that can interact with the modifying reagents. Unfortunately, the introduction of a serine or alanine residue in these positions completely deprived the mutants C74A/T290S and C74A/S295A of transport activity (data not shown), thus preventing us from testing whether their mutations expose endogenous cysteine residues.

To determine whether the reduced or completely absent transport activity of the cysteine mutants is due to an effect on function or defective targeting, their surface expression was tested by biotinylation. All of the mutants were correctly expressed on the cell surface with the exception of C74A/I292C, which showed reduced membrane expression (data not shown). The reduced or absent activity of the mutants, therefore, apparently cannot be ascribed to deficient plasma membrane expression, thus highlighting the importance of this region in the function of the transporter.

**Effect of sulfhydryl modification on the biophysical properties of the double C74A/T290C mutant.** Figure 7A shows the ability of this double mutant to give rise to transport-associated currents under control conditions: i.e. when 100 μM GABA was perfused before MTSET incubation. After treatment with the impermeant cysteine-modifying reagent, we did not observe a GABA-induced current but we did find a larger sodium leakage current at –40 mV membrane potential (fig. 7B), thus indicating a change in $Na^+$-transporter interaction. Statistical analysis showed a significant difference (fig. 7C) in the sodium leakage current before and after incubation with MTSET.

To clarify these effects further, we undertook a more detailed analysis by testing the behavior of transport-associated, transient and lithium leak currents under a wider range of voltages (figs. 8, 9). The C74A/T290C mutant showed WT-like behavior in terms of GABA apparent affinity (figs. 8A, 8B): by plotting the calculated concentration of GABA giving rise to half the maximal current ($K_{1/2\,(GABA)}$) at each potential versus the membrane potential (fig. 8B), we obtained a curve resembling that of the WT in terms of both voltage dependence and absolute values (i.e. about 10 μM at –40 mV) [see refs. 9, 40]. Incubation with MTSET abolished the transport-associated current at all voltages and GABA concentrations up to 3 mM (fig. 8A, filled symbols). Obviously, in this latter case, the apparent affinity for GABA could not be determined.

We also looked at the transient pre-steady-state currents in the C74A/T290C mutant before and after MTSET treatment (fig. 8C, D). A detailed analysis of these currents in a control solution containing 98 mM sodium confirmed WT-like behavior: fitting the sigmoid Q/V curve (empty squares in fig. 8E) with a Boltzmann function gave a $V_{1/2}$ value of $–27 \pm 2$ mV (n=8), similar to the WT value in the same batch ($–26 \pm 1$ mV, n=3, not shown). The analysis of the charge equilibration rate (empty squares in fig. 8F) also confirmed that the mutation did not alter the biophysical parameters of the transporter. MTSET treatment greatly impaired C74A/T290C tran-

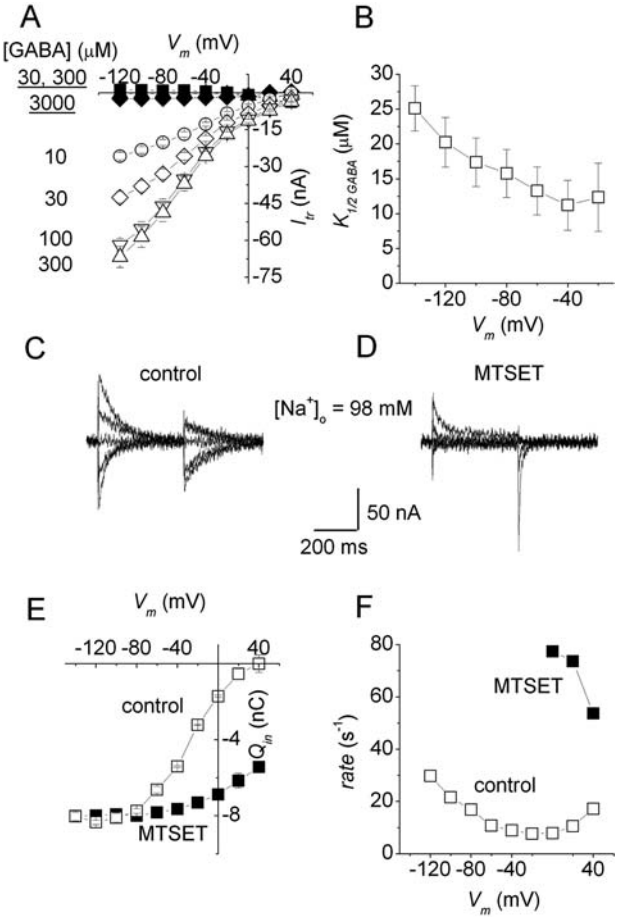


Figure 8. Biophysical characterization of the C74A/T290C double mutant. (*A*) Current *vs* voltage relationships of the transport-associated current elicited by the indicated GABA concentrations in GAT-1 C74A/T290C in $[Na^+]_o$=98 mM before (empty symbols) and after MTSET (filled symbols) treatment. Even at high GABA concentrations (underlined), no transport-associated current could be seen after MTSET treatment. (*B*) GABA apparent affinity evaluated under control conditions as the concentration giving rise to half $I_{tr}$ at each potential, resembling WT-like behavior [9]. Mean values ± SE of eight oocytes in both panels *A* and *B*. (*C*) and (*D*) Typical transient traces of the GAT-1 C74A/T290C double mutant before (*C*) and after (*D*) MTSET treatment recorded in an external solution containing 98 mM sodium. (*E*) Representative Q/V graph from the integration of the transient currents shown in panels *C* and *D* before (empty squares) and after (filled squares) MTSET treatment. Fitting the sigmoid of the Q/V curve with a Boltzmann function gave $V_{1/2}$ values of –27 ± 2 mV before treatment and +27 ± 8 mV after treatment (under control conditions, the $V_{1/2}$ for the WT form in the same batch was –26 ± 1 mV). The curves represent the mean values ± SE of the charge calculated from the integration of the 'on' and 'off' transients. The MTSET curve was arbitrarily shifted to match the control charge values at negative potentials. (*F*) Typical rate/V graph of the transient currents shown in panels *C* and *D* before (empty squares) and after (filled squares) MTSET treatment.

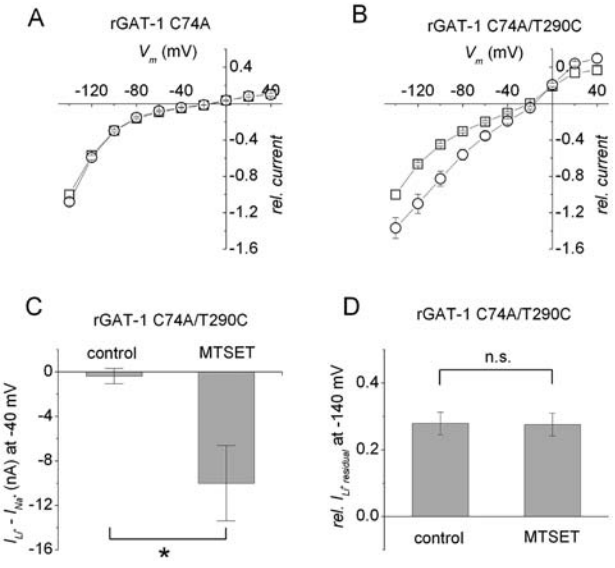


Figure 9. Lithium currents in the C74A and C74A/T290C mutants. Current vs voltage relationships of the C74A (*A*) and C74A/T290C (*B*) mutants before (squares) and after (circles) 15 min treatment with 2 mM MTSET. The recordings were made from the same oocytes and the current values were normalized at –140 mV before treatment. Mean values ± SE of 10 oocytes from two different donors. (*C*) Evaluation of lithium current (calculated as the difference between $I_{Li+}$ and $I_{Na+}$) under control conditions and after MTSET treatment (n=8) measured at fixed membrane potential (– 40 mV). (*D*) Evaluation of sodium-induced inhibition of lithium current in the double mutant. Oocytes expressing the C74A/T290C mutant were perfused with a solution containing 96 mM $Li^+$, and subsequently with a solution with 96 mM $Li^+$ and 2 mM $Na^+$ both before and after 15 min incubation with 2 mM MTSET. The residual lithium current was estimated by normalizing the current in the presence of 2 mM sodium to the value in its absence at –140 mV after subtraction in the presence of SKF89976A. The recordings were made from the same oocytes (n=8, two batches). The data in *C* and *D* were statistically analyzed using Student's t test: *, significantly different ($p < 0.05$); n.s., not significant.

sient currents, which could only be seen at depolarized potentials (fig. 8D). The results of the integration of these transients (plotted as filled squares in fig. 8E) have been arbitrarily shifted along the ordinate axis to match the charge value before MTSET treatment at negative potential. Although this Q/V curve is clearly far from reaching saturation at positive potential, there was a significant rightward shift of the sigmoid, with an estimated $V_{1/2}$ value of +27 ± 8 mV (filled squares in fig. 8E), and the alteration can also be seen in the rate of decay (filled squares in fig. 8F). This effect may be related to the increased $Na^+$ leak current shown in figure 7. Furthermore, a shift of the Q/V curve toward more positive potentials may be interpreted as an increase in sodium affinity [41]. To examine further whether MTSET incubation alters the interaction of the transporter with cations, we considered the lithium leak current. Like many other cotransporters of this family, GAT-1 also has uncoupled or leakage currents (i.e. transmembrane currents in the absence of organic substrate) that are best seen in the presence of lithium [22].

When lithium was perfused at a concentration of 98 mM, the mutated C74A/T290C transporter showed the same uncoupled current as the WT (not shown), thus confirm-

ing that the double mutations did not affect the function of the transporter. After incubation with MTSET, there was an increase in the lithium current at all tested potentials (circles in fig. 9B); the fact that this was not seen in the C74A mutant (fig. 9A) suggests that it is due to the MTSET-induced modification of the cysteine introduced in position 290. As shown in figure 9C, the increase in lithium current measured at –40 mV membrane potential was significantly different. The uncoupled lithium current exhibited by WT GAT-1 has been shown to be non-competitively inhibited by the presence of even small amounts of sodium ions, with an $IC_{50}$ of about 1.5 mM [12, 14, 42]. As we have shown that cysteine-modifying reagents alter the interaction of cations with the double-mutated transporter by increasing both sodium and lithium leakage currents, we further tested if sodium inhibition was altered by MTSET. The lithium currents were recorded from C74A/T290C-expressing oocytes before and after 15 min treatment with 2 mM MTSET, in both the absence and presence of 2 mM sodium. The sodium concentration was chosen because, as it is above the reported $IC_{50}$, it reduces the lithium current to about 30% of the control condition [14]. The analysis was made after subtracting the recording obtained in the presence of SKF89976A in 96 mM $Na^+$. For each experimental condition, the current values (in both the absence and presence of sodium) were normalized with respect to the value in control condition (96 mM $Li^+$ and absence of $Na^+$) at –140 mV. Figure 9C shows that, under control conditions, the presence of 2 mM $Na^+$ blocks the lithium leakage current to the same extent as in the WT. After MTSET treatment, this inhibition was not abolished or affected in any way, and the residual currents under the two conditions were not significantly different. Furthermore, the blockade was not significantly different when compared with the WT (data not shown). The introduction of bulk and charge by the MTSET-induced modification of position 290 therefore significantly increases the apparent affinity of the transporter for cations, but does not modify the non-competitive inhibition of lithium currents by sodium ions.

## Discussion

To identify the critical residues of GAT-1, we made a detailed analysis of about 250 amino acid sequences belonging to the family of $Na^+/Cl^-$-dependent neurotransmitter transporters, and found that one of the most conserved amino acids was the glutamine residue GAT-1 Q291 (fig. 1A), which is predicted to be located on the extracellular membrane surface (fig. 1B). All of our conservative and non-conservative mutations of Q291 abolished the function of GAT-1, as they showed no GABA transport (fig. 2) or any kind of current (fig. 3) even though they were sorted to the plasma membrane (fig. 2B). As the substitution or deletion of Q291 did not impair the cell surface targeting of GAT-1 in oocytes (fig. 2B) and cells (immunofluorescence experiments, data not shown), we can rule out defective targeting as the reason for the inactivity of the Q291 mutants. Furthermore, the involvement of Q291 in oligomerization can be excluded, because GAT-1 requires correct quaternary assembly for its efficient exit from endoplasmic reticulum and subsequent delivery to the plasma membrane [32, 34]. The fact that the Q291 mutants were expressed on the cell surface indicates that they form oligomers, and all of them showed the dimeric form of the protein even under experimental denaturing conditions (fig. 2B). Worth noting is that Hastrup et al. [33] replaced cysteines in TMD 6 at positions 317–321 (corresponding to GAT 291–295) in a cysteine-depleted dopamine transporter (DAT) construct, and found that the replacement of DAT Q317, F320 and S321 with cysteine was not tolerated because these constructs were not expressed at the cell surface (at least in the cysteine-depleted DAT background).

Although Q291 does not seem to be involved in oligomerization, our results do not rule out the possibility that it may promote the association of TM helices within the same monomer. As it is a hydrogen bond donor and acceptor, glutamine may interact with the polar residues of other TM helices and/or with substrates that could intervene as alternative hydrogen-bonding partners in place of other hydrophilic interactions [25].

With the exception of the glycine transporter (GLYT) [30], neurotransmitter transporters (such as GAT, the serotonin transporter SERT and DAT) exist in the membrane as dimers [31, 33, 43], or dimers of dimers [35]. Moreover, there is good evidence that the export of GAT-1 and other members of the family to the plasma membrane depends on oligomerization [32–34, 44, 45]. Mutant transporters in the membrane that lack transport activity can be used to investigate the functional role of the quaternary assembly of the protein by means of a functional approach based on coexpression experiments. Assuming that the assembly of monomeric proteins is a random process, and that only dimers of two WT monomers or tetramers of four WT monomers are functional, the coexpression of WT and correctly sorted non-functional mutants should affect WT transport activity. However, the data in figure 4 show that the coexpression of WT and correctly sorted non-functional GAT-1 mutants did not have any effect on GABA transport, thus suggesting that GAT-1 is fully functional as a monomer. Similar results were obtained when mutant expression was increased from 1:1 to 1:2. Sodium-coupled GABA transport therefore does not seem to require oligomerization [46], which is known to be important for protein stability and some aspects of membrane physiology, such as transporter trafficking and modulation. The atomic structure of LeuTAa is also consistent with the idea

that the monomer is the functional unit of the transporter because, although it forms a dimer in the crystal, each monomer has independent binding sites defined by transmembrane helices provided by the single monomer. In contrast, dominance effects have been observed in DAT [47] and SERT coexpression experiments [43], thus suggesting that oligomerization plays a functional role in such transporters. Furthermore, Seidel et al. [48] have demonstrated that the efflux and influx of organic substrates occur through distinct moieties within an oligomeric neurotransmitter transporter.

Mutants of the Q291 residue lack all transport activity, including the so-called pre-steady-state current that represents a partial and initial step in the transport cycle (figs. 2A, 3). This current is quantitatively related to the current coupled to the GABA transport and is believed to be strictly linked to the interaction of sodium with the transporter [41, 49]. As most of the proposed mechanistic models explaining the operational mode of GAT-1 assume that the first event is sodium binding [4, 22, 24, 38, 49], probably followed by conformational transitions that allow GABA recognition and transport, we speculated that the Q291 mutants may be unable to start the transport cycle because of their inability to recognize or bind sodium. It is worth noting that, defective GABA recognition cannot explain some of the experimental data, such as the lack of transient and leak currents in the Q291 mutants.

Given that none of the mutants were functional (including C74A/Q291C), we attempted to clarify the role of Q291 further by investigating the accessibility of some adjacent residues from the external milieu. The strong inhibition exerted by the impermeant MTS reagents on C74A/T290C and C74A/S295C (figs. 5, 6) suggests that the cysteine residues introduced into these mutants (respectively before and one helix turn below Q291) face the external aqueous environment or a water-filled cavity communicating with the external milieu.

These data are in agreement with the structure of the bacterial homologue solved by Yamashita et al. [26]. The residues corresponding to GAT Q291 and the other amino acids replaced by cysteine in the present study (figs. 1A, C) are located in the $LeuT_{Aa}$ in the external half of TMD 6 (called TM6a by Yamashita et al. [26]) or in the central, non-helical portion of TMD 6: in particular, the GAT positions that partially tolerate cysteine substitution (GAT-1 residues T290 and S295; fig. 5), correspond to G249 and T254 of $LeuT_{Aa}$. In the conformation of $LeuT_{Aa}$ reported by Yamashita et al. [26], G249 is located one helix turn above the leucine- and Na1 binding sites, and is likely to face the hydrophilic pathway leading to the binding sites, which would be in line with the external accessibility of the corresponding GAT T290 (fig. 6). $LeuT_{Aa}$ T254 is involved in the binding of both leucine and sodium, which is consistent with the fact that the corresponding GAT S295 is accessible from the external milieu (fig. 6). $LeuT_{Aa}$ F253 (corresponding to GAT F294, which does not tolerate cysteine replacement; fig. 5), is involved in the binding of leucine and is ultimately connected to $Na^+$ via a hydrogen bond network.

As shown in figures 6, 7 and 8, the sulfhydryl modification of GAT C74A/T290C, with its bulk and its charge, affected both transport-associated and pre-steady-state currents, and greatly impaired the transport of [$^3$H]GABA. It has to be noted that, apart from its reduced activity, the untreated double-mutated transporter behaved like the WT (fig. 8) but, after incubation with MTSET, its affinity for sodium was increased and the GABA-induced currents could no longer be seen. The positive shift observed in the Q/V curve (fig. 8E) after MTSET treatment is an indication of the greater apparent affinity of the transporter for sodium ions. The transporter seems to be locked in a particular step of the transport cycle (probably in the outward-facing conformation), an effect that is reminiscent of the W68L GAT-1 mutant studied by Mager et al. [22]. Obviously, in our case, the transporter cannot complete the cycle, and so we were unable to see transport-associated currents even in the presence of 3 mM GABA (figs. 7B, 8A), possibly because the steric hindrance and charge introduced by the MTSET modification does not allow the completion of the transport cycle, for example by preventing GABA binding or translocation. This hypothesis is supported by the structure reported by Yamashita et al. [26], which shows residue G249 (T290 in GAT) close to the leucine-binding site, and so the sulfhydryl modification of a cysteine introduced in this position may hamper the leucine binding.

The change in the behavior of C74A/T290C is consistent with the involvement of this residue in cation recognition or binding, as is also suggested by the increase in the uncoupled or leakage current after incubation with MTSET at a wide range of voltages (fig. 9).

The data presented in this work are compatible with the involvement of GAT Q291 in direct interaction with the cations and/or in maintaining the structural and functional integrity of an external region of the protein that makes it accessible to cations. The size of this water-filled cavity, which should be at least 6 Å wide, makes it too large to be a cation-binding site, regardless of whether the cation is hydrated or not, because the calculated molecular dimensions of MTSET and MTSES are respectively 11.5×6.0 Å and 12.0×6.0 Å [50]. However, as in $LeuT_{Aa}$ [51], GAT 290 and 295 could face a larger than expected water-accessible cavity that harbors the driving ion together with the driven GABA molecule.

Alternatively, as the correct positioning of the coordinating atoms is fundamental, Q291 may contribute to a hydrogen bond network that stabilizes various residues on the external surface of the transporter. This kind of structure could keep the transporter in an open conformation

capable of interacting with substrates. Possibly, the mutation of Q291 could make the transporter inaccessible to cations. However, whether the role of Q291 is to bind or direct the cations to inner domains of the protein, it is clear that it also involves other residues. We tested the possibility of a polar interaction between the highly conserved R69 of the extracellular half of TMD 1 [16] and Q291 but, unfortunately, the mutants R69Q/Q291R and R69L/Q291L did not show any recovery of activity in terms of GABA uptake or currents (data not shown).

The crystal structure of $LeuT_{Aa}$ solved by Gouaux's group represents a particular conformation during the transport cycle, when the binding pocket is occluded and the external and internal gates are closed. In this structure, Q250 (which corresponds to GAT Q291) is a key interacting residue at the extracellular gate of the transporter, and effectively part of a hydrogen bond network that ultimately connects Q250 to the sodium ion. Moreover, R30 (which corresponds to GAT R69) takes part in this same hydrogen bond network and interacts with Q250. Both the R30 and Q250 residues interact with other key residues on top of the binding pocket. In particular, R30 forms a water-mediated salt link with D404 of TMD 10. This explains why the GAT mutants R69Q/Q291R and R69L/Q291L do not recover any activity although the residues R69 and Q291 are probably spatially close and directly interact as in $LeuT_{Aa}$.

This crystal structure confirms that GAT Q291 is fundamental to maintaining the conformational integrity of an external region of the transporter that makes it accessible to the substrates, and we can speculate that it may even directly interact with the cations as the substrates move to the binding pocket. Other structures representing different transporter conformations will probably clear up this question. However, as Q291 is strictly conserved throughout the $Na^+/Cl^-$-dependent neurotransmitter transporter family, it is likely to play similar or related roles in all of these proteins.

*Acknowledgments*. The authors would like to thank Dr. S. Lin for critically reviewing the manuscript and K. Smart for his linguistic help. This research was funded by grants from the Italian Ministry of Research and University (FIRB program) to V. F. Sacchi for the project 'Investigation of protein structure and function by AFM and physiological studies' and to A. Peres for the project 'Sviluppo della metodologia FRET (Fluorescence Resonance Energy Transfer) per lo studio della funzionalità di trasportatori di neurotrasmettitori e amino acidi' (project No. RBAU01FKW2), and by a grant from Fondazione CARIPLO to A. Peres.

1 Guastella J., Nelson N., Nelson H., Czyzyk L., Keynan S., Miedel M. C. et al. (1990) Cloning and expression of a rat brain GABA transporter. Science **249:** 1303–1306
2 Palacìn M., Estévez R., Bertran J. and Zorzano A. (1998) Molecular biology of mammalian plasma membrane amino acid transporters. Physiol. Rev. **78:** 969–1054
3 Chen J. G., Liu-Chen S. and Rudnick G. (1998) Determination of external loop topology in the serotonin transporter by site-directed chemical labeling. J.Biol.Chem. **273:** 12675–12681
4 Mager S., Naeve J., Quick M., Labarca C., Davidson N. and Lester H. A. (1993) Steady states, charge movements, and rates for a cloned GABA transporter expressed in *Xenopus oocytes*. Neuron **10:** 177–188
5 Hilgemann D. W. and Lu C. C. (1999) GAT1 (GABA:$Na^+$:$Cl^-$) cotransport function. Database reconstruction with an alternating access model. J. Gen. Physiol. **114:** 459–475
6 Lu C. C. and Hilgemann D. W. (1999) GAT1 (GABA:$Na^+$:$Cl^-$) cotransport function. Kinetic studies in giant Xenopus oocytes membrane patches. J. Gen. Physiol. **114:** 445–457
7 Lu C. C. and Hilgemann D. W. (1999) GAT1 (GABA:$Na^+$:$Cl^-$) cotransport function. Steady state studies in giant Xenopus oocyte membrane patches. J. Gen. Physiol. **114:** 429–444
8 Bossi E., Giovannardi S., Binda F., Forlani G. and Peres A. (2003) role of anion-cation interactions in the pre-steady-state currents of the rat $Na^+$-$Cl^-$-dependent GABA cotransporters rGAT1. J. Physiol. **541:** 343–350
9 Fesce R., Giovannardi S., Binda F., Bossi E. and Peres A. (2002) The relation between charge movement and transport-associated currents in the GABA cotransporter rGAT1. J. Physiol. **545:** 739–750
10 DeFelice L. J., Adams S. V. and Ypey D. L. (2001) Single-file diffusion and neurotransmitter transporters: Hodgkin and Keynes model revisited. BioSystems **62:** 57–66
11 Loo D. D. F., Eskandari S., Boorer K. J., Sarkr H. K. and Wright E. M. (2000) Role of $Cl^-$ in electrogenic $Na^+$-coupled cotransporters GAT1 and SGLT1. J. Biol. Chem. **275:** 37414–37422
12 MacAulay N., Zeuthen T. and Gether U. (2002) Conformational basis for the $Li^+$-induced leak current in the rat γ-aminobutyric acid (GABA) trasporter-1. J. Physiol. **544:** 447–458
13 Golovanevsky V. and Kanner B. I. (1999) The reactivity of the γ-aminobutyric acid transporter GAT-1 toward sulfhydryl reagents is conformationally sensitive: identification of a major target residue. J. Biol. Chem. **274:** 23020–23026
14 Kanner B. I. (2003) Transmembrane domain I of the γ-aminobutyric acid transporter plays a crucial role in the transition between cation leak and transport modes. J. Biol. Chem. **278:** 3705–3712
15 Zomot E. and Kanner B. I. (2003) The interaction of the γ-aminobutyric acid transporter GAT-1 with the neurotransmitter is selectively impaired by sulphydryl modification of a conformationally sensitive cysteine residue engineered in extracellular loop IV. J. Biol. Chem. **278:** 42950–42958
16 Pantanowitz S., Bendahan A. and Kanner B. I. (1993) Only one of the charged amino acids located in the transmembrane α-helices of the γ-aminobutyric acid transporter (subtype A) is essential for its activity. J. Biol. Chem. **268:** 3222–3225
17 Keshet G. I., Bendahan A., Su H., Mager S., Lester H. A. and Kanner B. I. (1995) Glutamate-101 is critical for the function of the sodium and chloride-coupled GABA transporter GAT-1. FEBS Lett. **371:** 39–42
18 Sussman J. L., Harel M., Frolow F., Oefner C., Goldman A., Toker L. et al. (1991) Atomic structure of acetylcholinesterase from *Torpedo californica*: a prototypic acetylcholine-binding protein. Science **253:** 872–879
19 Gallivan J. P. and Dougherty D. A. (1999) Cation-pi interactions in structural biology. Proc. Natl. Acad. Sci. USA **96:** 9459–9464
20 Kavanaugh M. P., Hurst R. S., Yakel J., Varnum M. D., Adelman J. P. and North R. A. (1992) Multiple subunits of a voltage-dependent potassium channel contribute to the binding site for tetraethylammonium. Neuron **8:** 493–497
21 Kleinberger-Doron N. and Kanner B. I. (1994) Identification of tryptophan residues critical for the function and targeting of the g-aminobutyric acid transporter (subtype A). J. Biol. Chem. **269:** 3063–3067
22 Mager S., Kleinberger-Doron N., Keshet G. I., Davidson N., Kanner B. I. and Lester H. A. (1996) Ion binding and permeation at the GABA transporter GAT1. J. Neurosci. **16:** 5405–5414

23 Zomot E., Zhou Y. and Kanner B. I. (2005) Proximity of transmembrane domains 1 and 3 of the GABA transporter GAT-1 inferred from paired cysteine mutagenesis. J.Biol.Chem. **280:** 25512–25516

24 Bismuth Y., Kavanaugh M. P. and Kanner B. I. (1997) Tyrosine 140 of the g-aminobutyric acid transporter GAT-1 plays a critical role in neurotransmitter recognition. J. Biol. Chem. **272:** 16096–16102

25 Zhou F. X., Merianos H. J., Brunger A. T. and Engelman D. M. (2001) Polar residues drive association of polyleucine transmembrane helices. Proc. Natl. Acad. Sci. USA **98:** 2250–2255

26 Yamashita A., Singh S. K., Kawate T., Jin Y. and Gouaux E. (2005) Crystal structure of a bacterial homologue of $Na^+/Cl^-$-dependent neurotransmitter transporters. Nature **437:** 215–223

27 Mari S. A., Soragna A., Castagna M., Bossi E., Peres A. and Sacchi V. F. (2004) Aspartate 338 contributes to the cationic specificity and to driver-amino acid coupling in the insect cotransporter KAAT1. Cell. Mol. Life Sci. **61:** 243–256

28 Bennet E. R. and Kanner B. I. (1997) The membrane topology of GAT-1, a $(Na^+ + Cl^-)$-coupled g-aminobutyric acid transporter from rat brain. J. Biol. Chem. **272:** 1203–1210

29 Veenhoff L. M., Heuberger E. H. M. L. and Poolman B. (2002) Quaternary structure and function of transport proteins. Trends Biol. Sci. **27:** 242–249

30 Horiuchi M., Nicke A., Gomeza J., Ashrafi A., Schmalzing G. and Betz H. (2001) Surface-localized glycine transporters 1 and 2 function as monomeric proteins in *Xenopus* oocytes. Proc. Natl. Acad. Sci. USA **98:** 1448–1453

31 Schmid J. A., Scholze P., Kudlacek O., Freissmuth M., Singer E. A. and Sitte H. H. (2001) Oligomerization of the human serotonin transporter and of the rat GABA transporter 1 visualized by fluorescence resonance energy transfer microscopy in living cells. J. Biol. Chem. **276:** 3805–3810

32 Scholze P., Freissmuth M. and Sitte H. H. (2002) Mutations within an intramembrane leucine heptad repeat disrupt oligomer formation of the rat GABA transporter 1. J. Biol. Chem. **277:** 43682–43690

33 Hastrup H., Karlin A. and Javitch J. A. (2001) Symmetrical dimer of the human dopamine transporter revealed by cross-linking Cys-306 at the extracellular end of the sixth transmembrane segment. Proc. Natl. Acad. Sci. USA **98:** 10055–10060

34 Korkhov V. M., Farhan H., Freissmuth M. and Sitte H. H. (2004) Oligomerization of the g-aminobutyric acid transporter-1 is driven by an interplay of polar and hydrophobic interactions in transmembrane helix II. J. Biol. Chem. **279:** 55728–55736

35 Hastrup H., Sen N. and Javitch J. A. (2003) The human dopamine transporter forms a tetramer in the plasma membrane: cross-linking of a cysteine in the fourth transmembrane segment is sensitive to cocaine analogs. J. Biol. Chem. **278:** 45045–45048

36 Just H., Sitte H. H., Schmid J. A., Freissmuth M. and Kudlacek O. (2004) Identification of an additional interaction domain in transmembrane domains 11 and 12 that supports oligomer formation in human serotonin transporter. J. Biol. Chem. **279:** 6650–6657

37 Yu N., Cao Y., Mager S. and Lester H. A. (1998) Topological localization of cysteine 74 in the GABA transporter, GAT1, and its importance in ion binding and permeation. FEBS Lett. **426:** 174–178

38 Zhou Y., Bennet E. R. and Kanner B. I. (2004) The aqueous accessibility in the external half of transmembrane domain I of the GABA transporter GAT-1 is modulated by its ligands. J. Biol. Chem. **279:** 13800–13808

39 Hirokawa T., Boon-Chieng S. and Mitaku S. (1998) SOSUI: classification and secondary structure prediction system for membrane proteins. Bioinformatics **14:** 378–379

40 Forlani G., Bossi E., Ghirardelli R., Giovannardi S., Binda F., Bonadiman L. et al. (2001) Mutation K448E in the external loop 5 of rat GABA transporters rGAT1 induces pH sensitivity and alters substrate interactions. J. Physiol. **536:** 479–494

41 Soragna A., Bossi E., Giovannardi S., Pisani R. and Peres A. (2005) Relations between substrate affinities and charge equilibration rates in the rat GABA cotransporter GAT1. J. Physiol. **562:** 333–345

42 Grossman T. R. and Nelson N. (2003) Effect of sodium lithium and proton concentrations on the electrophysiological properties of the four mouse GABA transporters expressed in *Xenopus* oocytes. Neurochem. Int. **43:** 431–443

43 Kilic F. and Rudnick G. (2000) Oligomerization of serotonin transporter and its functional consequences. Proc. Natl. Acad. Sci. USA **97:** 3106–3111

44 Farhan H., Korkhov V. M., Paulitschke V., Dorostkar M. M., Scholze P., Kudlacek O. et al. (2004) Two discontinuous segments in the carboxyl terminal are required for membrane targeting of the rat g-aminobutyric acid transporter-1 (GAT-1). J. Biol. Chem. **279:** 28553–28563

45 Sitte H. H. and Freissmuth M. (2003) Oligomer formation by $Na^+$-$Cl^-$-coupled neurotransmitter transporters. Eur. J. Pharmacol. **479:** 229–236

46 Soragna A., Bossi E., Giovannardi S., Pisani R. and Peres A. (2005) Functionally independent subunits in the oligomeric structure of the GABA cotransporter rGAT1. Cell. Mol. Life Sci. **23:** 2862–2870

47 Torres G. E., Carneiro A., Seamans K., Fiorentini C., Sweeney A., Yao W.-D. et al. (2003) Oligomerization and trafficking of the human dopamine transporter: mutational analysis identifies critical domains important for the functional expression of the transporter. J. Biol. Chem. **278:** 2731–2739

48 Seidel S., Singer E. A., Just H., Farhan H., Scholze P., Kudlacek O. et al. (2005) Amphetamines take two to tango: an oligomer-based counter-transport model on neurotransmitter transport explores the amphetamine action. Mol. Pharmacol. **67:** 140–151

49 Peres A., Giovannardi S., Bossi E. and Fesce R. (2004) Electrophysiological insights into the mechanism of ion-coupled cotransporters. News Physiol. Sci. **19:** 80–84

50 Kaplan R. S., Mayor J. A., Brauer D., Kotaria R., Walters D. E. and Dean A. M. (2000) The yeast mitochondrial citrate transport protein: probing the secondary structure of transmembrane domain IV and identification of residues that likely comprise a portion of the citrate translocation pathway. J. Biol. Chem. **275:** 12009–12016

51 Kanner B. I. (2005) Molecular physiology: intimate contact enables transport. Nature **437:** 203–205

52 Persson B. and Argos P. (1994) Prediction of transmembrane segments in proteins utilising multiple sequence alignments. J. Mol. Biol. **237:** 182–192

53 Krogh A., Larsson B., Heijne G. von and Sonnhammer E. L. (2001) Predicting transmembrane protein topology with a hidden Markov model: application to complete genomes. J. Mol. Biol. **305:** 567–580

54 Tusnady G. E. and Simon I. (2001) The HMMTOP transmembrane topology prediction server. Bioinformatics. **17:** 849–850

55 Cserzo M., Wallin E., Simon I., Heijne G. von and Elofsson A. (1997) Prediction of transmembrane alpha-helices in prokaryotic membrane proteins: the dense alignment surface method. Protein Eng. **10:** 673–676

56 Hofmann K. and Stoffel W. (1993) TMbase – a database of membrane spanning protein segments. Biol. Chem. Hoppe-Seyler **374:** 166–168

57 Jones D. T., Taylor W. R. and Thornton J. M. (1994) A model recognition approach to the prediction of all-helical membrane protein structure and topology. Biochemistry **33:** 3038–3049

58 Pasquier C. and Hamodrakas S. J. (1999) An hierarchical artificial neural network system for the classification of transmembrane proteins. Protein Eng. **12:** 631–634